Mass Transfer and Weld Appearance of 316L Stainless Steel Covered Electrode During Shielded Metal Arc Welding

ZHAOLING DUAN, RENYAO QIN, and GUO HE

The mass transfer and the weld appearance of 316L stainless steel covered electrodes during shielded metal arc welding were investigated. According to the experimental measurements on the deposited metal and the observations on the welding process, the mass transfer coefficient of the nickel was found to be in the range of 88.09 to 99.41 pct, while those of molybdenum, chromium, manganese, and silicon are in the ranges of 84.60 to 92.51 pct, 71.59 to 77.64 pct, 20.88 to 30.15 pct, and 6.72 to 10.47 pct, respectively. Some relationships between the mass transfer and the flux coating ingredient/welding current were established. The formability properties of the weld, including the spreadability, spattering, slag detachability, and oxidation tint on the weld surface, were also discussed based on the tested data and the observations.

I. INTRODUCTION

STAINLESS steels were widely used in chemical equipment and power generation as structural supports, containers, pipes, *etc.* because of their good corrosion resistance. In stainless steel catalogue, austenitic stainless steels comparatively have both good mechanical properties, particularly ductility and toughness, and acceptable workability, formability, and weldability; thus, they were extensively used in welded structure or weld assembly.[1] Because of the relatively low heat conductivity and high thermal expansion, the austenitic stainless steels require special welding precautions and appropriate welding materials as filler metals so as to prevent welding distortion, residual stresses, and weld defects in either the weld bead or the heat-affected zone (HAZ).[1,2] Apart from weld forming, the chemical composition of the weld metal (depending on the filler metal and the welding process) is extremely important for maintaining adequate mechanical properties and high corrosion resistance. For shielded metal arc welding (SMAW), the metal mass transfer from the covered electrode to the weld pool depends crucially on the flux ingredient coated on the electrode and the welding parameters.[3,4] This definitively determines the final chemical composition of the weld. Although one can empirically estimate the mass transfer during SMAW, the relatively accurate transfer coefficients of the key elements (*i.e.*, Ni, Cr, and Mo) in the stainless steel covered electrodes, especially for the newly developed ones with faintly acidic flux coatings that bring the good weld quality and easy welding operation together, are practically useful for welding engineering design and welding material development.

Traditionally, the flux coating on the electrodes is either "rutile type" or "basic type."[3] The former is mainly composed of TiO_2, Al_2O_3, SiO_2, and carbonates with which a very stable welding process can be achieved; the latter principally consists of CaF_2, MgO, carbonates, and silicates. With such a coating ingredient, the crack sensitivity will be reduced because the hydrogen in the weld can be controlled in a very low level.[3] In recent years, the development of the flux coating ingredient has tended to take advantage of both the rutile type and basic type, forming a new type composed of TiO_2, SiO_2, Al_2O_3, and CaF_2. With the help of this new flux coating, we developed some stainless steel covered electrodes that have both a stable welding process and a high weld quality (especially the impact resistance performance). However, the mass transfer of the key elements in such new flux coating is unclear. What factors contribute to the mass transfer coefficients and the weld formability for such new covered electrodes? These problems need to be experimentally investigated.

In this article, we focused on a 316L austenitic stainless steel covered electrode (according to the classification of AWS A5.4/A5.4M). The aim was to investigate the mass transfer of the key elements Si, Mn, Cr, Ni, and Mo during SMAW. The special emphasis was put on the weld formability and the oxidation tint on the weld surface, which were related to the flux coating and the welding current according to the experimental measurements and the observations. The mass transfer and some metallurgical phenomena that occurred during SMAW were discussed.

ZHAOLING DUAN, Master Student, RENYAO QIN, Doctoral Student, and GUO HE, Professor, are with the State Key Lab of Metal Matrix Composites, School of Materials Science and Engineering, Shanghai Jiao Tong University, Shanghai 200240, P.R. China. Contact e-mail: ghe@sjtu.edu.cn
Manuscript submitted February 1, 2013.
Article published online October 30, 2013.

II. MATERIALS AND EXPERIMENTAL PROCEDURE

The stainless steel covered electrodes were fabricated in our partner welding material factory according to the general manufacture process. The composition of the

core wire with dimensions of o.d. 4.0 mm × 35 mm was listed in Table I. The flux coating bonded by water glass consisted of a mixture of carbonates, oxides, fluorides, and metal powders. For the sake of cost saving, the pure compounds and oxides were replaced by some commercial mineral powders such as marble, fluorite, mica, feldspar, cryolite, and rutile. All the mineral and metal powders used in the experiment were sieved by using a mesh size of 450 μm. According to the experimental purpose, the coating ingredients were specially designed and could be divided into several groups, as listed in Table II. The names Current-1, Current-2, and Current-3 in the table denote the welding currents set to 90 A, 130 A, and 170 A, respectively, for the Current-group electrodes. The basicity of slag for each flux coating was evaluated according to the following equation:[5]

$$B = \frac{1.8CaO + 1.4(K_2O + Na_2O) + 0.6CaF_2}{1.7SiO_2 + 0.5TiO_2} \quad [1]$$

All the oxides and fluorites in the equation are in weight percent. When $B > 1$, the slag is alkaline; when $B < 1$, the slag is acidic; and when $B = 1$, the slag is neutral.

After they were coated, the covered electrodes were dried at temperature steps of 313 K, 393 K, and 623 K for 2 hours total in order to avoid cracking of the coating layer. A time inverter DC arc welding machine WS-400 (PNE50-400, Mingpu Machinery Co., Ltd., Shanghai) was applied to perform the welding operation with the following parameters: welding current = 130 A, welding voltage = 32 to 36 V, welding speed = 4 mm/s, and arc length = 1 to 3 mm. The heat input was estimated to be in the range of 0.78 to 0.88 KJ/mm (when the welding current = 90 A, the heat input was in the range of 0.54 to 0.61 KJ/mm; when the welding current = 170 A, the heat input was in the range of 1.02

to 1.15 KJ/mm). The entire welding operation was carried out by a professional welder in the same manner to avoid operating error. The covered electrodes were melted on a 316L stainless steel plate. The weld pad for the chemical analysis of the undiluted weld metal was prepared according to the specification AWS A5.4/ A5.4M. The weld pad size was length = 50 mm, width = 16 mm, and height = 30 mm. The chemical composition of the deposited metal was analyzed using the Thermo Scientific (Shanghai, China) inductively coupled plasma emission spectrometer (iCAP 6300 ICP).

The mass transfer from the covered electrodes to the weld pad during SMAW could be depicted quantitatively using following equation:[4,6]

$$\eta = \frac{C_{depo}}{C_{wire} + k_b C_{coating}} \quad [2]$$

where η is the mass transfer coefficient; C_{depo} indicates the weight percent of the target element in the deposited metal; C_{wire} and $C_{coating}$ denote the weight percents of this element in the core wire and the flux coating, respectively; and k_b is the weight ratio of the flux coating to the core wire in the covered electrode. Since the weight percents of each designated element in the wire and the coating are known, one can directly determine the mass transfer coefficients if the composition of the deposited metal is determined.

The bead spreadability, the slag detachability, and the oxidation extent of the weld surface are very important characteristic parameters that indicate the welding quality and the operability of the covered electrodes. The bead spreadability can be measured by the bead width, which was determined directly from the weld photos. Since only the relative values among the comparative welds were sought in this investigation, all the photos were taken at the same amplification. When doing the measurement, two parallel straight lines

Table I. Chemical Composition of the Core Wire (Weight Percent)

C	S	P	Si	Mn	Cr	Ni	Mo	Cu	Fe
0.030	0.002	0.018	0.13	2.18	19.22	11.74	2.27	0.04	balance

Table II. Coating Ingredients of the Stainless Steel Covered Electrodes (in Weight Proportions)

Number	CaCO$_3$	Na$_2$CO$_3$	CaF$_2$	Na$_3$AlF$_6$	SiO$_2$	Al$_2$O$_3$	K$_2$O	Ni	Mo	TiO$_2$	Mn	Cr	Fe
CaCO$_3$-1	**6.0**	1.0	4.0	1.0	30.5	4.0	9.5	1.0	1.0	32.0	1.5	8.0	1.0
CaCO$_3$-2	**12.0**	1.0	4.0	1.0	30.5	4.0	9.5	1.0	1.0	32.0	1.5	8.0	1.0
CaCO$_3$-3	**18.0**	1.0	4.0	1.0	30.5	4.0	9.5	1.0	1.0	32.0	1.5	8.0	1.0
Mn-1	9.0	1.0	4.0	1.0	30.5	4.0	9.5	2.0	1.0	32.0	**5.0**	22.0	1.0
Mn-2	9.0	1.0	4.0	1.0	30.5	4.0	9.5	2.0	1.0	32.0	**8.0**	22.0	1.0
Mn-3	9.0	1.0	4.0	1.0	30.5	4.0	9.5	2.0	1.0	32.0	**12.0**	22.0	1.0
Cr-1	9.0	1.0	4.0	1.0	30.5	4.0	9.5	2.0	1.0	32.0	5.0	**22.0**	1.0
Cr-2	9.0	1.0	4.0	1.0	30.5	4.0	9.5	2.0	1.0	32.0	5.0	**26.0**	1.0
Cr-3	9.0	1.0	4.0	1.0	30.5	4.0	9.5	2.0	1.0	32.0	5.0	**30.0**	1.0
Ni-1	9.0	1.0	4.0	1.0	30.5	4.0	9.5	**2.0**	1.0	32.0	5.0	22.0	1.0
Ni-2	9.0	1.0	4.0	1.0	30.5	4.0	9.5	**6.0**	1.0	32.0	5.0	22.0	1.0
Ni-3	9.0	1.0	4.0	1.0	30.5	4.0	9.5	**10.0**	1.0	32.0	5.0	22.0	1.0
Current	18.0	1.0	4.0	1.0	30.5	4.0	12	1.0	1.0	32.0	1.5	8.0	1.0

Bold values indicate the independent variable.

were drawn along the two side boundaries of the weld on the photos (only measuring the middle stable welding bead because the initial and ending welding was unstable). The lines should overlap with the boundaries as much as possible. The distance of the two parallel straight lines was taken as the bead width.

The oxidation extent of the weld surface can be roughly evaluated by the oxidation tint. It has already been established that the stainless steel discolors from pale yellow at 563 K (290 °C) to brown at 663 K (390 °C) and dark blue at 873 K (600 °C) when heating in the air due to thermal oxidation.[7–10] The weld oxides formed in varied oxidizing environments at various temperatures have different compositions and thus exhibit different colors.[11,12] It is clear that the lower temperature and the weaker oxidizing environment result in light color, but the higher temperature and the stronger oxidizing environment cause deep color (e.g., violet blue observed in this study). For SMAW, the key factor is the crucial temperature at which the slag gets detached from the weld. Once the slag peels off, the fresh weld metal will expose in air, and oxidation will occur. The peeling-off temperature depending on the flux coating ingredients of the covered electrodes and the welding parameters determines the oxidation extent of the weld surface (i.e., colors on the surface). Thus, the color code can be used to evaluate if the slag provides good protection and peels off at the appropriate temperature.

III. RESULTS

A. Mass Transfer Coefficients of the Stainless Steel Covered Electrodes

The compositions of the deposited metals of all the covered electrodes prepared in this study were collected in Table III. The mass transfer coefficients of the Si, Mn, Cr, Ni, and Mo in the covered electrodes could be calculated according to Eq. [2] by using the data listed in Tables I through III. They were summarized in Table IV. These data present a sketch-map (as shown in Figure 1) that intuitively reveals the range of the mass transfer coefficients of different elements in the stainless steel covered electrodes during SMAW. The Si has the lowest mass transfer coefficient of around 8.6 pct, while the Ni demonstrates the highest mass transfer coefficient of about 93.75 pct. The other elements Mo, Cr, and Mn are ranked in the middle. Their mass transfer coefficients are around 88.56, 74.62, and 25.52 pct, respectively. Therefore, the mass transfer coefficients of the five elements in the stainless steel covered electrodes can be ranked in the following order: $\eta_{Ni} > \eta_{Mo} > \eta_{Cr} > \eta_{Mn} > \eta_{Si}$.

B. Effect of Basicity on the Mass Transfer Coefficient and the Weld Appearance

The basicity of the flux coating depends on the relative proportion of each oxide and fluoride in the coating. Since CaO is a strong basic oxide, the $CaCO_3$ group (Table II) was designed to investigate the effect of the basicity on the mass transfer coefficient and weld appearance, in which the $CaCO_3$ portion was set to be 6, 12, and 18 pct, respectively. The basicity of slag corresponds successively to 0.57, 0.67, and 0.77 (calculated by using Eq. [1]), as noted in Table IV. Although the basicity of slag varies in such a small range, the mass transfer coefficients of Si, Mn, Cr, Ni, and Mo display some changes, as shown in Figure 2. The mass transfer coefficients of Cr, Mo, and Ni slightly increase as the basicity increases from 0.57 to 0.77 (Figure 2(a)), whereas those of Si and Mn exhibit the opposite tendency (Figure 2(b)). Obviously, the mass transfer coefficients of Cr, Mo, Ni, and Si are insensitive to the change of the basicity. The percentage of the Cr mass transfer coefficient only increases by 1.06 as the basicity increases from 0.57 to 0.77. And the percentages of the Ni and Mo mass transfer coefficients increase by 1.17 and 1.34, respectively. In contrast, the percentage of the

Table III. Chemical Compositions of the Deposited Metals of the Stainless Steel Covered Electrodes (Weight Percent) (Welding Current = 130 A)

Number	C	S	P	Si	Mn	Cr	Mo	Ni	Fe
$CaCO_3$-1	0.025	0.004	0.022	0.57	0.90	18.78	2.46	12.04	balance
$CaCO_3$-2	0.027	0.005	0.026	0.56	0.82	18.56	2.44	12.17	balance
$CaCO_3$-3	0.032	0.007	0.021	0.43	0.62	18.55	2.53	12.21	balance
Mn-1	0.03	0.007	0.0221	0.62	**1.19**	21.96	2.49	11.95	balance
Mn-2	0.03	0.008	0.019	0.61	**1.66**	22.03	2.54	11.52	balance
Mn-3	0.033	0.007	0.020	0.71	**2.24**	21.96	2.36	11.31	balance
Cr-1	0.03	0.007	0.0221	0.62	1.19	**21.96**	2.49	11.95	balance
Cr-2	0.03	0.008	0.02	0.65	1.27	**22.66**	2.49	13.41	balance
Cr-3	0.028	0.008	0.022	0.61	1.34	**23.85**	2.51	11.39	balance
Ni-1	0.03	0.007	0.0221	0.62	1.19	21.96	2.49	**11.16**	balance
Ni-2	0.03	0.008	0.02	0.65	1.27	22.66	2.49	**13.92**	balance
Ni-3	0.024	0.008	0.0222	0.55	1.26	20.89	2.45	**16.05**	balance
Current-1*	0.031	0.007	0.031	0.41	0.80	18.55	2.43	11.93	balance
Current-2	0.032	0.007	0.021	0.42	0.74	18.44	2.44	12.04	balance
Current-3**	0.037	0.008	0.024	0.43	0.62	18.32	2.46	12.08	balance

Bold values indicate the significant change in the chemical compositions.
*Welding current = 90 A.
**Welding current = 170 A.

Table IV. Element Mass Transfer Coefficients of the Stainless Steel Covered Electrodes

Number	η_{Si} (Pct)	η_{Mn} (Pct)	η_{Cr} (Pct)	η_{Mo} (Pct)	η_{Ni} (Pct)	Notes (Difference in the Coating Compositions or in the Welding Current)
CaCO$_3$-1	8.72	29.49	76.58	87.54	98.24	CaCO$_3$ = 6 wt-p; B = 0.57
CaCO$_3$-2	8.30	27.24	76.74	87.85	98.80	CaCO$_3$ = 12 wt-p; B = 0.67
CaCO$_3$-3	6.99	20.88	77.64	88.88	99.41	CaCO$_3$ = 18 wt-p; B = 0.77
Mn-1	8.54	25.76	73.30	85.88	93.97	Mn = 5 wt-p
Mn-2	8.80	27.73	74.21	92.51	90.77	Mn = 8 wt-p
Mn-3	10.47	29.25	75.05	84.60	89.39	Mn = 12 wt-p
Cr-1	8.54	25.76	73.30	85.88	93.97	Cr = 22 wt-p
Cr-2	9.49	28.46	72.89	91.33	92.62	Cr = 26 wt-p
Cr-3	9.10	30.15	72.70	92.18	90.07	Cr = 30 wt-p
Ni-1	8.54	25.76	73.30	85.88	88.09	Ni = 2 wt-p
Ni-2	9.49	28.46	72.89	91.33	92.62	Ni = 6 wt-p
Ni-3	8.21	28.35	71.59	89.98	93.97	Ni = 10 wt-p
Current-1	6.72	27.00	77.64	87.48	97.36	welding current = 90 A
Current-2	6.99	25.20	77.16	87.85	98.24	welding current = 130 A
Current-3	7.12	20.88	76.69	88.58	98.63	welding current = 170 A

wt-p: in weight proportion.
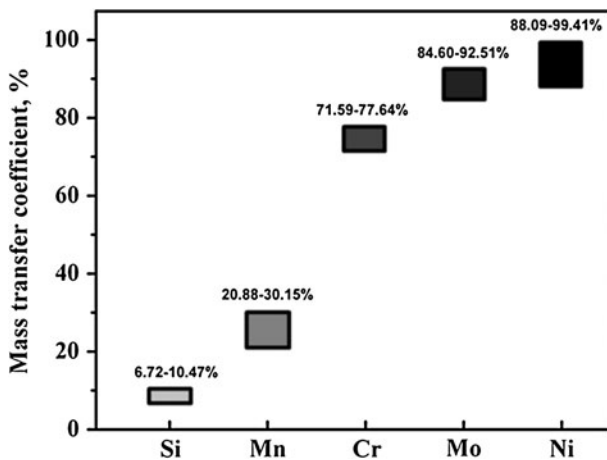
Fig. 1—Range of the mass transfer coefficients of the 316L stainless steel covered electrodes.

Si mass transfer coefficient decreases by 1.73 as the basicity increases to the same extent. The Mn is more sensitive to the basicity. Its mass transfer coefficient declines significantly as the basicity increases. When the basicity is 0.57, the Mn mass transfer coefficient reaches 29.49 pct, but this value is reduced to 20.88 pct when the basicity increases to 0.77.

The weld appearance shows some relation to the basicity. Comparing the weld beads carefully, one can find that the width of the weld beads becomes narrower as the basicity increases (CaCO$_3$ increases in the coating), indicating that the spreadability of the molten metal during SMAW becomes worse, as shown in Figure 3. Besides, the three weld beads obviously show an oxidation tint that indicates the protective efficiency of the flux coating. The weld bead of CaCO$_3$-1 looks violet blue, suggesting not-so-good protection. But the weld bead of CaCO$_3$-3 has a normal metal color with little pale blue stains, indicating very good protection. It

is clear that the oxidation on the weld surface becomes weak as the basicity increases from 0.57 to 0.77. In other words, the flux coating with higher basicity (more CaCO$_3$ in the coating) provides better protection for the weld beads.

C. Effect of the Metal Contents in the Coating on the Mass Transfer Coefficient and the Weld Appearance

The groups of Mn-1 to Mn-3, Cr-1 to Cr-3, and Ni-1 to Ni-3 (Table II) were intended to identify the effect of the contents of the Mn, Cr, and Ni on their mass transfer coefficients and the weld appearance. All the ingredients listed previously were designed in the same basicity for easy evaluation. The three metals tested in this study clearly showed that the mass transfer coefficients were dependent on the metal contents in the coating. Particularly, the Mn and Ni contents in the coating affected the mass transfer coefficients significantly, as shown in Figures 4(a) and (b). The increase in the Mn content in the coating from 5 to 12 (in weight proportion) led to the increase in its mass transfer coefficient from 25.76 to 29.25 pct. The Ni demonstrated a similar behavior, i.e., the mass transfer coefficient increased from 88.09 to 93.97 pct as its content in the coating increased from 2 to 10 (in weight proportion). Unlike Mn and Ni, the Cr mass transfer coefficient decreased from 73.30 to 72.70 pct as its content in the coating increased from 22 to 30 (in weight proportion), as shown in Figure 4(c). Considering the experimental error, it seemed that the Cr mass transfer coefficient was insusceptible of the Cr content in the coating.

Since Mn has a lower melting point, a lower surface tension of the molten metal in the weld pool can be expected at higher Mn content, which should lead to higher spreadability of the molten metal and wider weld bead. But, in this study, no obvious difference in the bead width was observed as the Mn content in the coating increased from 5 to 12 (in weight proportion).

The Ni also had no influence on the bead width as its content in the coating increased from 2 to 10 (in weight proportion). However, some difference among the weld beads could be detected when changing the Cr content in the coating. The weld bead of Cr-3 was obviously thinner than that of the other two weld beads, as shown
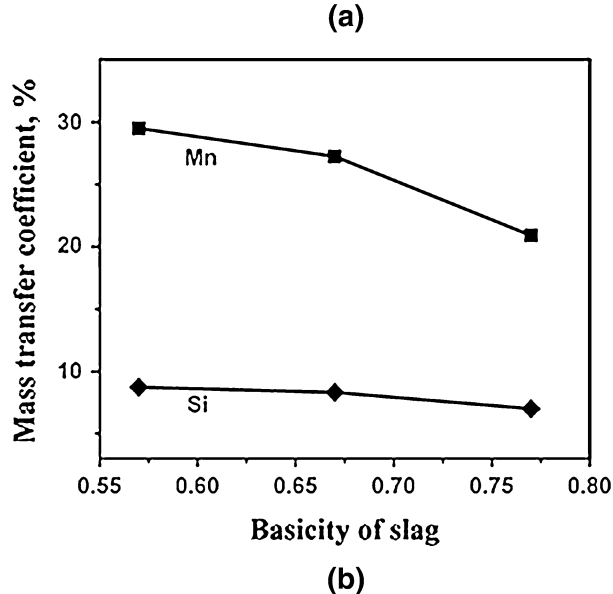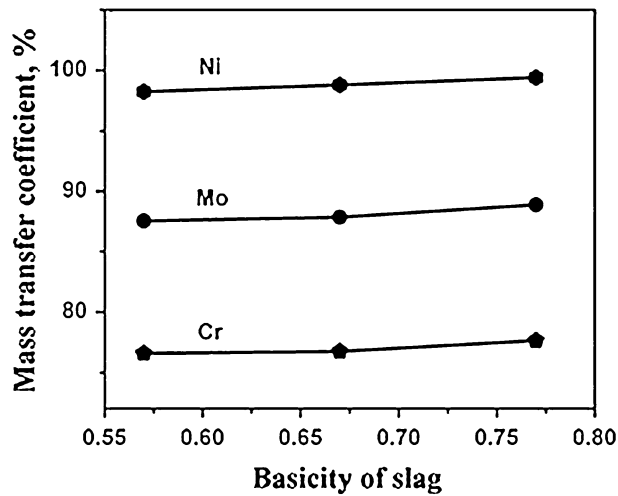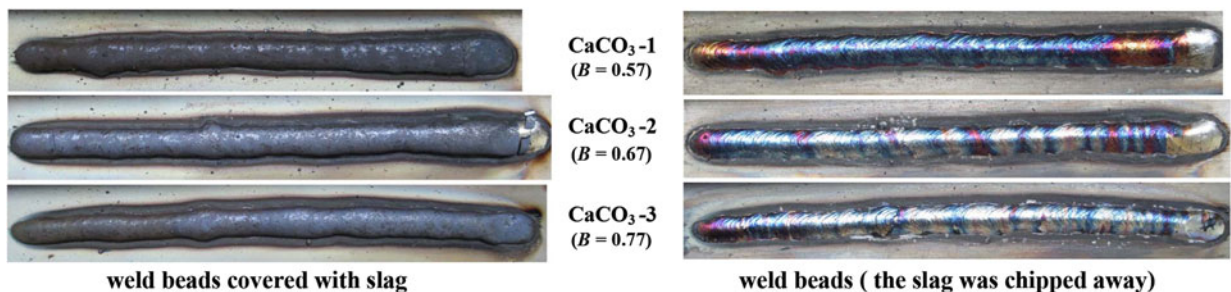
in Figure 5, suggesting that the Cr content of 30 (in weight proportion) led to lower flowability and spreadability of the molten metal. Furthermore, the weld bead of Cr-1 showed violet blue color; that of Cr-2 looked pale blue with some dark yellow zones; and that of Cr-3 was straw yellow with some normal metal color. It was clear that the oxidation on the weld surface became weak as the Cr content increased in the coating.

D. Effect of Welding Current on the Mass Transfer Coefficient and the Weld Appearance

In order to evaluate the effect of welding current on the mass transfer coefficients of the stainless steel covered electrodes, the coating ingredient, named "Current" in Table II, was designed and has a very good balance of stable welding process and weld quality. Three different welding currents, 90, 130, and 170 A, were applied in the welding operation. 130 A is generally in the range of the proposed welding current for this type of covered electrode. But 90 and 170 A are below and beyond the proposed welding current range, respectively. With such large steps of welding current, all the target elements in the covered electrode showed that their mass transfer coefficients were somewhat dependent on the welding current, as shown in Figure 6. Particularly, the Mn mass transfer coefficient was significantly affected by the welding current, which decreased from 27 to 20.88 pct as the welding current increased from 90 to 170 A (Figure 6(b)). The Cr also had a similar decreasing tendency in its mass transfer coefficient as the welding current was increased, but the decreasing amplitude was small, as shown in Figure 6(d). The other three elements, Si, Mo, and Ni, exhibited a reverse changing tendency in their mass transfer coefficients as the welding current was increased, as shown in Figures 6(a), (c), and (e). However, the increasing amplitudes of the mass transfer coefficients for all three elements were small, i.e., $\Delta\eta_{Si} = 0.4$ pct, $\Delta\eta_{Mo} = 1.1$ pct, and $\Delta\eta_{Ni} = 1.27$ pct. For easy reference, all of the mass transfer coefficients are summarized in Table IV.

The effect of welding current on the weld appearance was distinct, as shown in Figure 7. Welding with 130 A resulted in a very good balance of the stable arc combustion, excellent slag detachability, fine appearance of weld, and suitable bead width. As expected,

Fig. 2—Effect of the basicity of slag on the mass transfer coefficient of the 316L stainless steel covered electrodes.

Fig. 3—Weld images of the 316L stainless steel covered electrodes with different basicity of slag, showing the slag (left) and the deposited metal (right).
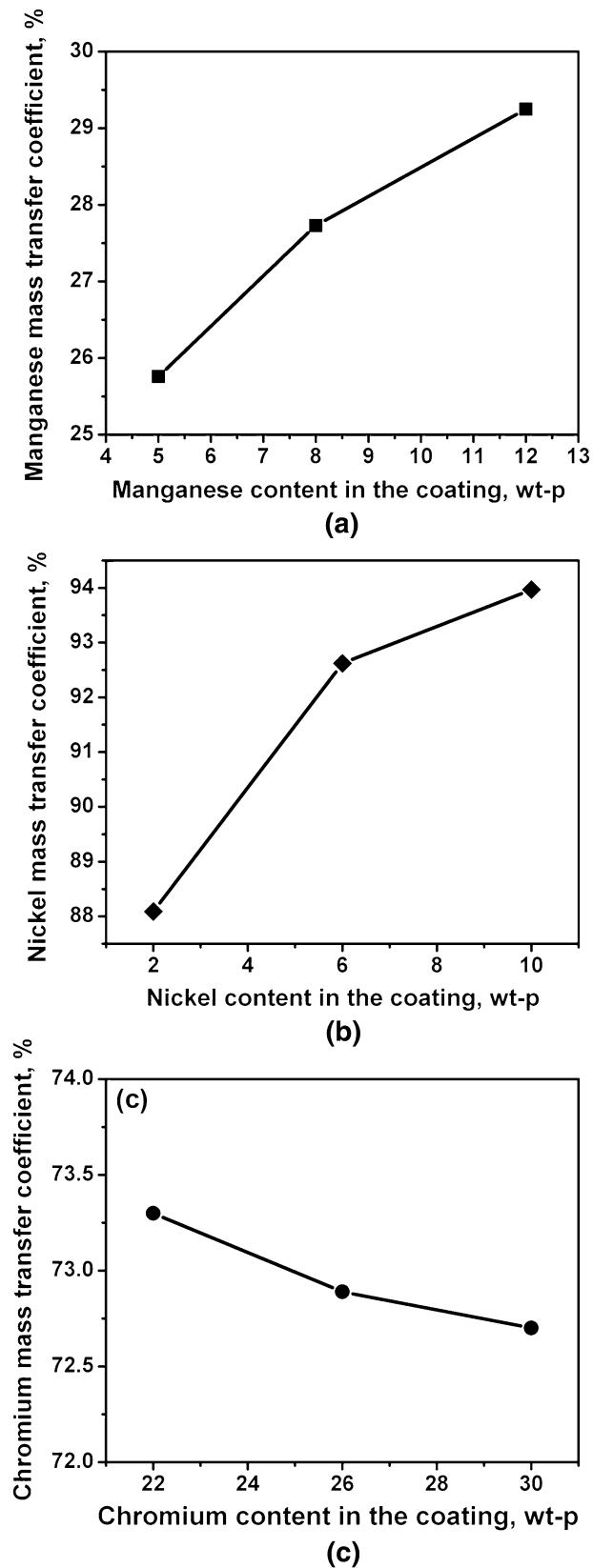
(a)

(b)

(c)

Fig. 4—Effect of the metal content on the mass transfer coefficient of the 316L stainless steel covered electrodes.

welding with a small current (*e.g.*, 90 A) led to a narrow weld bead because of the small heat input (0.54 to 0.61 KJ/mm). This generally resulted in lower temperature in the weld pool that increased the viscosity of the molten metal and reduced its spreadability. Welding with large current (*e.g.*, 170 A) led to a wide weld bead because of the large heat input (1.02 to 1.15 KJ/mm). Compared with the former (welded with 90 A), the latter (welded with 170 A) increased the bead width by 54 pct, because the large heat input could overheat the molten metal and increase its spreadability. However, the large current induced violent spatters (indicated by white arrows in Figure 7) and unstable arc combustion. This might result in a poor appearance of the weld (refer to the partial enlarged view in Figure 7). Besides, the large current also induced worse slag detachability. Some burnt-on slag could be observed on the weld, as indicated by the black arrows in Figure 7.

In addition, the different welding current also led to different slag color. When welding with 90 A, the slag looked near dark brown. But when welding with 170 A, the slag was dark gray. It was believed that the heat input (controlling the temperature in the weld pool) determined the metallurgical reaction. Large or small heat input (corresponding to the metallurgical reaction at high or low temperature, respectively) must result in the different slag products with different compositions and ingredients, which could be either acidic or near neutral. The slag formed during SMAW with 90 A provided poor protection of the weld metal from oxidation, so that the weld metal looked dark violet with some blue zones, as shown in Figure 7. The weld metal formed with 130 A showed a normal metal color with some pale blue stains, indicating good protection from the oxidation. Although the weld metal formed with 170 A also had a normal metal color in some areas, the oxidation on the surface was significant according to overall observation on the weld metal, as shown in Figure 7.

IV. DISCUSSION

A. *Mass Transfer During SMAW for the Stainless Steel Covered Electrodes*

All the elements in the stainless steel covered electrodes (including those in the core wire and the flux coating) can be either deposited into the weld bead or oxidized into the slag. Some of the elements may be partially evaporated or burnt off, forming spatters into the surroundings. How much into the weld bead depends on the chemical and physical properties of each element and the metallurgical reaction occurring during SMAW. The Cr, Ni, and Mo are key alloying metals in the stainless steel. It is desirable for the majority of these metals in the stainless steel covered electrode to be transferred into the weld bead and very few lost (*i.e.*, transferred into the slag or the surroundings). In fact, the Ni and Mo in the covered electrodes could be efficiently transferred into the weld bead
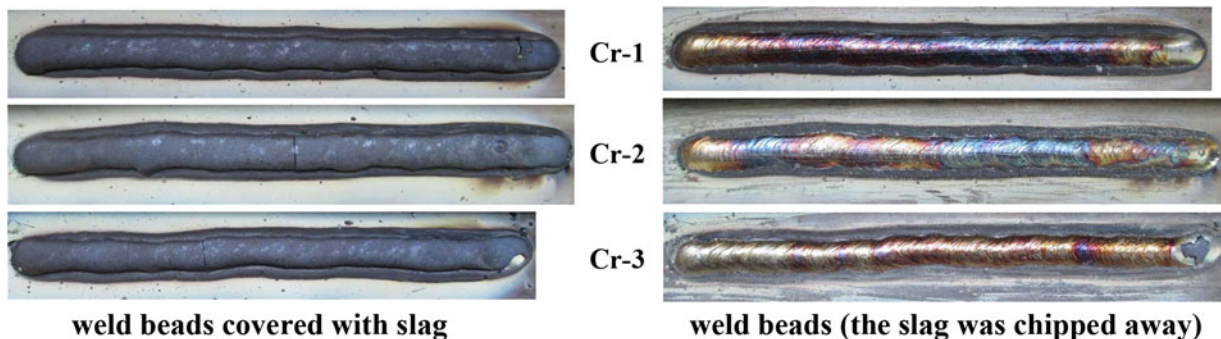
Fig. 5—Weld images of the 316L stainless steel covered electrodes with different Cr content in the flux coating, showing the slag (left) and the deposited metal (right).

according to the experimental data in this investigation. Their mass transfer coefficients reached 88 to 99 pct and 84 to 92 pct, respectively, indicating that their loss was relatively small. The Cr, however, revealed considerable loss so that its mass transfer coefficient was only 71 to 77 pct. If simply considering their oxidizing loss, the difference in the transfer coefficients among the three metals can be easily understood. Generally, the temperature can reach up to 2400 K (2127 °C) in the arc zone and 2000 K (1727 °C) in the weld pool during SMAW.[3,6] At such high temperature, the three metals could be oxidized by O_2, CO_2, water vapor, and other oxidizers decomposed from the flux coating. How much was oxidized depends mainly on their affinity for oxygen at the welding temperature. It is known that the oxygen affinity of the three metals can be ranked from weak to strong in the order of Ni < Mo < Cr at the welding temperature according to the Ellingham diagram,[13] so that it is reasonable that $\eta_{Ni} > \eta_{Mo} > \eta_{Cr}$. This is entirely in accord with the experimental results.

The Mn in the stainless steel covered electrodes (in both the core wire and the flux coating) plays a dual role both as an alloying metal and a deoxidizer in the metallurgical process during SMAW, because it has a stronger affinity for oxygen than Fe and other alloying metals such as Ni, Mo, and Cr.[13–15] If the Mn transfers into the weld bead, it acts as an alloying metal, contributing to the value of the Mn mass transfer coefficient. Otherwise, it acts as a deoxidizer to form oxide entering slag. This will reduce the Mn mass transfer coefficient. According to this investigation, it could be estimated that about 21 to 30 pct Mn in the stainless steel covered electrodes transferred into the weld bead as an alloying metal and about 70 to 79 pct Mn acted as a deoxidizer entering the slag.

Just like Mn, Si is also an alloying element that can transfer into the weld bead from both the core wire and the flux coating. But the Si in the coating generally acts as the deoxidizer and slag former, because it has a much stronger affinity for oxygen than Fe and the other four metals discussed previously.[13–15] Only about 6 to 10 pct Si transferred into the weld bead and more than 90 pct Si entered the slag according to this study (Figure 1). Although only a small part of the Si became the alloying element, the "Si rise" in the weld bead was significant (compared to the Si content in the core wire, as

indicated in Table I, with that in the weld bead, as listed in Table III). It is clear that the Si in the compounds or oxides in the coating can transfer into the weld bead during SMAW for the stainless steel covered electrodes with such acidic coating ingredients. Such an effect must be considered in the coating ingredient design or the welding operation with the stainless steel covered electrodes.

B. Effect of Coating Ingredients on the Mass Transfer Coefficient and the Weld Appearance

The flux coating is the mixture of the minerals and the metal powders. Any changes in the coating ingredients may affect the basicity of the slag and the metallurgical reaction during SMAW. Among the ingredients, some strong basic or acidic oxides (e.g., CaO and SiO_2) play key roles in creating a good balance between the welding process and the weld quality. When increasing $CaCO_3$ in the coating, the basicity and oxidability of the slag increase because of the following reaction:

$$CaCO_3 \rightarrow CaO + CO_2 \qquad [3]$$

The CO_2 gas protects the weld pool from air. Otherwise, it is also a strong oxidizing gas at high temperature.[6,16] In the welding metallurgical reactions, the CO_2 gas may primarily oxidize Si and Mn, because both elements have stronger affinity for oxygen than Fe, Ni, Mo, and Cr,[13–15] resulting in the decrease of the Si and Mn in the weld bead. This mechanism can help to understand why the Si and Mn mass transfer coefficients decreased significantly as the basicity of slag increased (i.e., $CaCO_3$ in the coating increased), as shown in Figure 2(a).

The CaO is strongly basic and acts as the arc stabilizer and the molten steel purification agent for desulfurization and dephosphorization by following reactions:[17,18]

$$FeS + CaO \rightarrow CaS + FeO \qquad [4]$$

$$P_2O_5 + 3CaO \rightarrow Ca_3P_2O_8 \qquad [5]$$
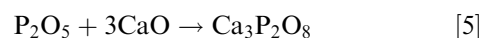
In addition, the CaO can keep a chemical balance with the strong acidic oxide SiO_2 and other acidic oxides in such a complex metallurgical reaction system. As the
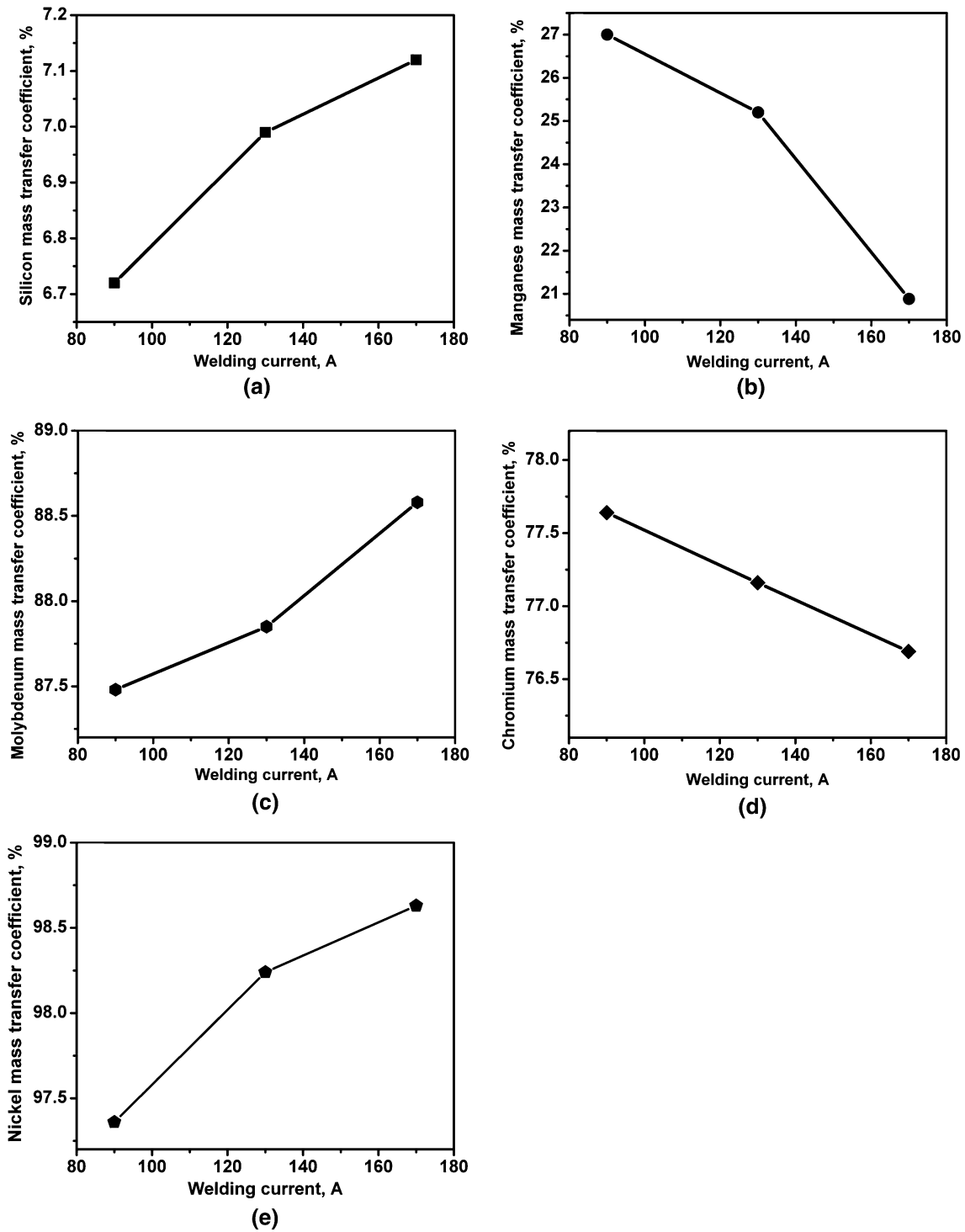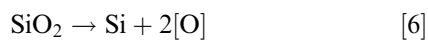
Fig. 6—Effect of welding current on the mass transfer coefficient of the 316L stainless steel covered electrodes.

CaO increases, the following decomposition reaction can be restrained:

$$SiO_2 \rightarrow Si + 2[O] \qquad [6]$$

This again reduces the Si mass transfer coefficient. In contrast, Cr_2O_3 and NiO are basic oxides in acidic circumstance.[5,6] Their decomposition reactions at high temperature can be enhanced as the strong basic CaO increases:

$$Cr_2O_3 \rightarrow 2Cr + 3[O] \qquad [7]$$
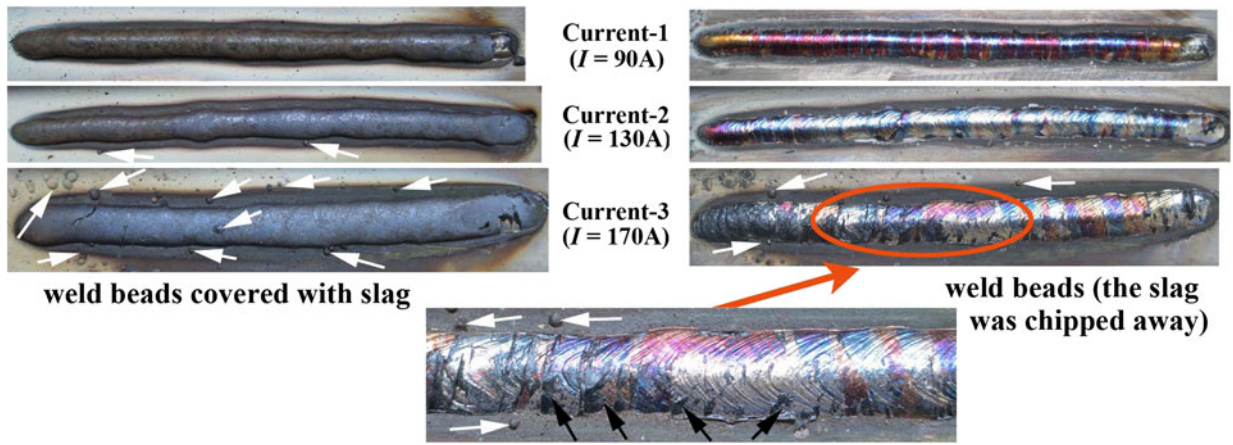
$$NiO \rightarrow Ni + [O] \qquad [8]$$

Fig. 7—Weld images of the 316L stainless steel covered electrode welded under three different welding currents, showing the slag (left), the deposited metal (right), and the local amplified image of the weld metal (bottom).

Consequently, the Cr and Ni mass transfer coefficients increase as the basicity of slag increases, as shown in Figure 2(b). The Mo is believed to have a similar behavior because its affinity for oxygen is between Fe and Cr.[13–15]

Besides, the weld beads become narrow as the $CaCO_3$ in the coating increases, as shown in Figure 3, indicating that the fluidity of the melts in the weld pool becomes worse. This can be attributed to the SiO_2 in the slag, which, reacting with O^{2-}, can form Si-O anions, such as SiO_4^{4-}, $Si_6O_{16}^{6-}$, or $Si_9O_{21}^{6-}$, because the greater amount of CaO corresponds to the greater amount of SiO_2 in the slag due to the chemical balance between the basic and acidic oxides, as stated previously. The Si-O anion with complex structure and large dimension would cause a high viscosity of slag, blocking the molten weld metal underneath from spreading properly.[5]

The oxidation tint on the weld beads depends on the temperature at which the slag peels off spontaneously or is chipped away. The violet blue color forms around 773 K to 873 K (500 °C to 600 °C), but the pale yellow or metal color forms below 573 K (300 °C),[8–10] which means that the peeling-off of the slag occurs at an early stage (at relatively high temperature) for the $CaCO_3$-1 (Table II). As the basicity of slag increases, the peeling-off of the slag occurs at relatively low temperature; thus, the oxidation tint becomes light, as shown in Figure 3. In addition, as the $CaCO_3$ in the coating increases, the CO_2 gas formed by the $CaCO_3$ disintegrating increases. More CO_2 gas may provide better protection for the weld metal.

When the basicity of slag is constant, the Mn and Ni mass transfer coefficients increase as their proportions in the coating increase, as shown in Figures 4(a) and (b). This is because the oxidative substance in the certain weld metallurgical process is relatively definite. It can be exhausted by a certain amount of reductive elements such as Si and Mn. The excess Mn and Ni can transfer into the weld, increasing their mass transfer coefficients.

It is as expected that the Cr in the deposited metal increases from 21.96 to 23.85 pct (Table III) as it increases in the coating from 22 to 30 (in weight proportion). But the Cr mass transfer coefficient seems insensitive to the changes of the Cr proportion in the coating (Figure 4(c) and Table IV). Such behavior is different from that of the Mn and Ni. It is believed that the chromium oxides that enter the slag will increase as the Cr in the coating increases. The Cr_2O_3 (melting temperature: 2708 K (2435 °C)) may be infusible at the welding temperature and will increase the viscosity of the molten slag, leading to thick slag.[6] Obviously, the thick slag enfolds more Cr_2O_3 and reduces the spreadability of the weld melts. This certainly decreases the Cr mass transfer coefficient and deteriorates the slag covering on the weld, as shown in Figure 5. According to the oxidation tint on the weld beads (Figure 5), increasing Cr in the coating delays the peeling-off of the slag, so that the weld color changes in turn from violet blue to pale blue and straw yellow.

C. Effect of Welding Current on the Mass Transfer Coefficient and the Weld Appearance

Welding with the current in the range of 100 to 150 A (for 4-mm-diameter stainless steel covered electrodes) is often suggested by the welding materials producers. A current below 100 A can only be recommended for horizontal or overhead position welding, and that above 150 A is merely adopted when the welding velocity and deposition efficiency are dominantly pursued. Welding with large current certainly generates large heat input and leads to a relatively high welding temperature,[19] which influences the welding metallurgical reactions and in turn affects the mass transfer coefficient and the welding quality. It is known that the droplet transfer mode during arc welding tends to transform from projected spray to streaming spray as the welding current increases.[20] The two modes generate different droplet sizes, as illustrated in Figure 8. The smaller droplets together with the higher arc temperature generally have more chances to be oxidized. As a result, the Mn and Cr mass transfer coefficients decrease as the welding current increases, as shown in Figures 6(b) and (d), because they have stronger affinity for oxygen than
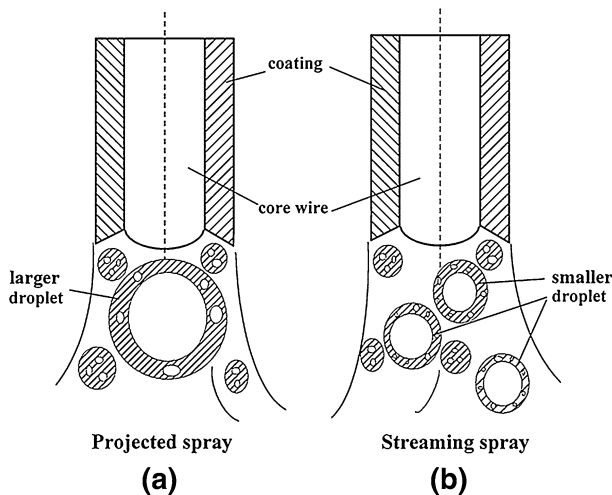
Fig. 8—Illustration of the droplet transfer modes.

the other metals. The Ni and Mo have weaker oxygen affinity than Mn and Cr, so they avoid oxidation (Figures 6(c) and (e)). It should be noted that Mn is the most sensitive to the welding current. Apart from its stronger affinity for oxygen, the Mn evaporation at high temperature also contributes to the reduction of its mass transfer coefficient because the boiling point of Mn is relatively low. Regarding Ni and Mo, there is another concern that their mass transfer mode is mainly adopted by the core wire transfer, which remains insensitive to the surrounding circumstance and results in higher mass transfer coefficients than those obtained by the coating transfer.[4]

The Si transfer occurs partially from the core wire, but the Si rise in the deposited metal is believed to come from the decomposition of SiO_2 in the flux coating. The high arc temperature can improve the SiO_2 decomposition reaction (Eq. [6]) because of its high decomposition pressure at high temperature.[6,21] Thus, the Si mass transfer coefficient exhibits an increasing tendency as the welding current increases from 90 to 170 A, as shown in Figure 6(a).

It is ordinary that the weld bead becomes wider when increasing the welding current, as shown in Figure 7. This is because the higher temperature (corresponding to the larger welding current) can reduce the viscosity of the slag[5,6] and improve the spreadability of the molten metals. When a large welding current is applied, many more electrons emitted from the striking end will impact the particles in the arc zone. Meanwhile, the high temperature (induced by the large welding current) will intensify the gas-phase reaction in the arc zone (Eq. [3]). These dual effects evidently lead to spattering, as indicated by white arrows in Figure 7.

The worst slag detachability occurs when welding with a current of 170 A. The remaining slags likely attach between the weld ripples, as shown in Figure 7. It is evident that the weld ripple is distinct and rough when welding with 170 A. The rough weld surface is believed to easily adhere to slag. Another concern is that the greater number of Cr_2O_3 compounds caused by the stronger oxidizing atmosphere will react with the

bivalent oxides (such as MnO and FeO) to form spinels.[22] The crystal structure of the spinels is similar to that of the weld metal, causing the spinels to firmly adhere to the weld metal.[23] Both of the effects account for the poor slag detachability.

According to the findings in this investigation and the preceding discussion, one can establish a general criterion for keeping a high mass transfer coefficient for the three major metals Ni, Cr, and Mo. The higher basicity of slag is beneficial for increasing its mass transfer coefficients. The Ni can be added in the flux coating, because the high mass transfer coefficient can be achieved in this way. But it is preferential to add the Cr to the core wire, because the Cr in the flux coating will experience a greater loss than that in the core wire during welding. In addition, the higher welding current can increase the mass transfer coefficients of Ni and Mo, but decrease that of Cr.

V. CONCLUSIONS

Based on the special coating ingredient design and experimental measurement, the mass transfer coefficients of the 316L stainless steel covered electrodes during SMAW were quantitatively evaluated. The key factors to govern the transfer coefficients and the weld formability were comprehensively investigated. The following conclusions can be drawn.

1. When welded under the operating current of 130 A, the Ni mass transfer coefficient is in the range of 88.09 to 99.41 pct, the Mo in the range of 84.60 to 92.51 pct, the Cr in the range of 71.59 to 77.64 pct, the Mn in the range of 20.88 to 30.15 pct, and the Si in the range of 6.72 to 10.47 pct. They can be ranked in the following order: $\eta_{Ni} > \eta_{Mo} > \eta_{Cr} > \eta_{Mn} > \eta_{Si}$. Although the Si mass transfer coefficient is relatively small, the Si rise in the deposited metal is significant for all the tested samples.
2. As the basicity of slag increases, the mass transfer coefficients of Cr, Mo, and Ni slightly increase, but those of Si and Mn decrease. The Mn transfer is comparably much more sensitive to the change of the basicity. In addition, the basicity of slag influences the spreadability of the molten metal and the slag detachability. As the basicity of slag increases, both the spreadability and the slag detachability become worse, but the surface oxidation of the weld bead becomes weak because the peeling-off of the slag can be delayed.
3. The mass transfer coefficients of Mn and Ni increase as their contents in the flux coating increase. But that of Cr demonstrates a reverse tendency. Its mass transfer coefficient decreases slightly when its content in the flux coating increases from 22 to 30 in weight proportion. Besides, the greater amount of Cr in the flux coating results in the worse spreadability of the molten metal and delays the peeling-off of the slag.
4. The mass transfer coefficients of Cr, Mo, Ni, and Si are insensitive to the welding current. But the Mn

transfer can be reduced significantly when increasing the welding current. The welding with a small current (*i.e.*, 90 A) results in worse spreadability of the molten metal. The welding with a very large current (*i.e.*, 170 A) causes poor slag detachability and evidently spattering. The welding with 130 A leads to a good balance of the stable welding process, excellent slag detachability, and fine appearance of weld.

REFERENCES

1. J.C. Lippold and D.J. Kotecki: *Welding Metallurgy of Stainless Steels*, 1st ed., John Wiley & Sons Inc., Hoboken, NJ, 2005, pp. 1–229.
2. M. Turski, J.A. Francis, P.R. Hurrell, S.K. Bate, S. Hiller, and P.J. Withers: *Int. J. Press. Vess. Pip.*, 2012, vol. 89, pp. 9–18.
3. C. Bonnet: in *Metallurgy and Mechanics of Welding*, R. Blondeau, ed., John Wiley & Sons, Hoboken, NJ, 2008, pp. 169–204.
4. R. Qin and G. He: *Metall. Mater. Trans. A*, 2013, vol. 44A, pp. 1475–84.
5. H. Liu: *Welding Metallurgy and Weldability*, Machinery Industry Press, Beijing, 2007, pp. 59–64 (in Chinese).
6. W. Zhang: *Welding Metallurgy*, Machinery Industry Press, Beijing, 1999, pp. 55–57 (in Chinese).
7. P.K. Rastogi, B.K. Shah, A.K. Sinha, and P.G. Kulkarni: *Br. Corr. J.*, 1994, vol. 29, pp. 178–80.
8. *AWS D18.2 Guide to Weld Discoloration Levels on Inside of Austenitic Stainless Steel Tube*, American Welding Society, Miami, FL, 2009.
9. E.M. Westin, C.-O.A. Olsson, and S. Hertzman: *Corr. Sci.*, 2008, vol. 50, pp. 2620–34.
10. C. Powell and D. Jordan: *Fabricating Stainless Steels for the Water Industry*, Reference Book, Series No.11026, Nickel Institute, Durham, NC.
11. S. Turner and F.P.A. Robinson: *Corrosion*, 1989, vol. 49, pp. 710–16.
12. K. Asami and K. Hashimoto: *Corr. Sci.*, 1979, vol. 19, pp. 1007–17.
13. H.J.T. Ellingham: *J. Soc. Chem. Ind.*, 1944, vol. 63, pp. 125–33.
14. F.D. Richardson and J.H.E. Jeffes: *J. Iron Steel Res. Int.*, 1948, vol. 160, pp. 261–70.
15. N.N. Greenwood and A. Earnshaw: *Chemistry of the Elements*, 2nd ed., Butterworth–Heinemann, Oxford, United Kingdom, 1997, pp. 328–61 and 1040–62.
16. S. Kou: *Welding Metallurgy*, 2nd ed., John Wiley & Sons, Hoboken, NJ, 2003, pp. 65–98.
17. Y. Nakajima and M. Mukai: *ISIJ Int.*, 1993, vol. 33, pp. 109–15.
18. S. Nakamura, F. Tsukihashi, and N. Sano: *ISIJ Int.*, 1993, vol. 33, pp. 53–58.
19. Md.I. Khan: *Weld. Sci. Technol.*, 1st ed., New Age International Ltd., New Delhi, 2007, pp. 69–96.
20. R.W. Messler: *Principles of Welding*, Wiley-VCH Verlag GmbH & Co. KGaA, Weinheim, 2004, pp. 270–90.
21. D. Starodub, E.P. Gusev, E. Garfunkel, and T. Gustafsson: *Surf. Rev. Lett.*, 1999, vol. 6, pp. 45–52.
22. H. Li and W. Chen: *Corr. Sci.*, 2010, vol. 52, pp. 2481–88.
23. Q. Zhang: *The Theory and Technology of Welding Material*, Metallurgical Industry Press, Beijing, 2002, pp. 85–86.